

Table 2A. Soil Parameters for HS-small Analysis of Sec 1-1 (To be Continued)

Soil layer	Layer thickness (m)	Soil type	γ_{unsat} (kN/m ³)	γ_{sat} (kN/m ³)	k (m/day)	c_{ref} (kN/m ²)	Φ (°)	Ψ (°)
#1	0.9	SF	16.9	20.0	2.0×10^{-4}	0.2	28	0
#2	5.2	SM	17.3	20.6	5.0×10^{-4}	0.3	29	0
#3	9.8	SM	16.0	19.9	5.0×10^{-3}	0.3	30	0
#4	12.4	CL	14.8	19.1	5.0×10^{-1}	0.5	27	0
#5	4.1	SM	15.9	19.3	5.0×10^{-3}	0.3	32	2
#6	5.1	CL	14.7	19.0	5.0×10^{-3}	0.5	31	1
#7	11.0	SM	15.7	19.4	5.0×10^{-3}	0.3	33	3
#8	4.8	CL	15.8	19.9	5.0×10^{-3}	0.5	31	1
#9	1.6	SM	15.9	19.5	5.0×10^{-3}	0.3	33	3
#10	5.1	GM	16.9	21.0	8.64	0.1	35	5

Table 2B. Soil Parameters for HS-small Analysis of Sec 1-1 (Continued)

Soil layer	Layer thickness (m)	Soil type	E_{50}^{ref} (kN/m ²)	E_{oed}^{ref} (kN/m ²)	E_{ur}^{ref} (kN/m ²)	ν	ν_{ur}	G_0^{ref} (kN/m ²)	$\gamma_{0.7}$	m
#1	0.9	SF	12,500	-	-	0.35	-	-	-	-
#2	5.2	SM	20,000	-	-	0.34	-	-	-	-
#3	9.8	SM	30,000	-	-	0.33	-	-	-	-
#4	12.4	CL	13,200	13,200	39,600	-	0.15	85,063	1.85×10^{-4}	1
#5	4.1	SM	47,500	-	-	0.32	-	-	-	-
#6	5.1	CL	26,400	26,400	79,200	-	0.15	94,313	2.03×10^{-4}	1
#7	11.0	SM	62,500	-	-	0.32	-	-	-	-
#8	4.8	CL	30,000	30,000	90,000	-	0.15	126,533	1.25×10^{-4}	1
#9	1.6	SM	97,500	-	-	0.32	-	-	-	-
#10	5.1	GM	12,500	-	-	0.30	-	-	-	-

Selection of Soft Soil Creep Model Parameters

The time-dependent behavior of soil is considered in the Soft Soil Creep model. The change of stiffness with stress is simulated during compression. Parameters required for the analysis include:

c : Cohesion [kN/m²];

ϕ : Friction angle [°];

Ψ : Dilatancy angle [°];

λ^* : Modified compression index;

κ^* : Modified swelling index;

μ^* : Modified creep index;

ν_{ur} : Poisson's ratio for unloading-reloading; $\nu_{ur}=0.15$ for the study;

K_o^{NC} : Stress ratio in a state of normal consolidation;

M : K_o^{NC} -related parameter (see below); and

e_{init} : Initial void ratio.

The modified compress index, λ^* , modified swelling index, κ^* and modified creep index, μ^* , are determined using the formulas below, where c_c , c_r and c_α are the coefficient of compressibility, coefficient of re-compressibility and coefficient of secondary compressibility, respectively. The stress ratio in a state of normal consolidation, K_o^{NC} , is calculated using Jaky's formula, $K_o^{NC}=1-\sin\phi$. For the soft soil creep model, the value of K_o^{NC} has influence on the slope of critical state line, M , which is calculated as follows:

$$\lambda^* = \frac{c_c}{2.3(1+e)}$$

$$\kappa^* = \frac{c_r}{2.3(1+e)}$$

$$\mu^* = \frac{c_\alpha}{2.3(1+e)}$$

$$M = 3 \sqrt{\frac{(1 - k_0^{NC})^2}{(1 + 2k_0^{NC})^2} + \frac{(1 - k_0^{NC})(1 - 2v_{ur})(\lambda^*/\kappa^* - 1)}{(1 + 2k_0^{NC})(1 - 2v_{ur})\lambda^* - (1 - k_0^{NC})(1 + v_{ur})}}$$

Table 3 provides the soil parameters entered for Soft Soil Creep model analysis of cross section 1-1 based on the requirements and recommendations above.

Table 3A. Soil Parameters for SSC Analysis of Sec 1-1 (To be Continued)

Soil layer	Layer thickness (m)	Soil type	γ_{unsat} (kN/m ³)	γ_{sat} (kN/m ³)	k (m/day)	c_{ref} (kN/m ²)	Φ (°)	Ψ (°)
#1	0.9	SF	16.9	20.0	2.0×10^{-4}	0.2	28	0
#2	5.2	SM	17.3	20.6	5.0×10^{-4}	0.3	29	0
#3	9.8	SM	16.0	19.9	5.0×10^{-3}	0.3	30	0
#4	12.4	CL	14.8	19.1	5.0×10^{-1}	0.5	27	0
#5	4.1	SM	15.9	19.3	5.0×10^{-3}	0.3	32	2
#6	5.1	CL	14.7	19.0	5.0×10^{-3}	0.5	31	1
#7	11.0	SM	15.7	19.4	5.0×10^{-3}	0.3	33	3
#8	4.8	CL	15.8	19.9	5.0×10^{-3}	0.5	31	1
#9	1.6	SM	15.9	19.5	5.0×10^{-3}	0.3	33	3
#10	5.1	GM	16.9	21.0	8.64	0.1	35	5

Table 3B. Soil Parameters for SSC Analysis of Sec 1-1 (Continued)

Soil layer	Layer thickness (m)	Soil type	κ^*	λ^*	μ^*	e	v	v_{ur}	k_0^{NC}
#1	0.9	SF	-	-	-	-	0.35	-	-
#2	5.2	SM	-	-	-	-	0.34	-	-
#3	9.8	SM	-	-	-	-	0.33	-	-
#4	12.4	CL	0.0233	0.0788	0.0042	0.81	-	0.15	0.546
#5	4.1	SM	-	-	-	-	0.32	-	-
#6	5.1	CL	0.0179	0.0596	0.0032	0.74	-	0.15	0.485
#7	11.0	SM	-	-	-	-	0.32	-	-
#8	4.8	CL	0.0200	0.0677	0.0036	0.54	-	0.15	0.485
#9	1.6	SM	-	-	-	-	0.32	-	-
#10	5.1	GM	-	-	-	-	0.30	-	-

NUMERIC ANALYSIS RESULTS VS. IN-SITU MONITORING DATA

The following are the results of Hardening Soil model with small-strain stiffness and Soft Soil Creep model based on the numeric analysis method and requirements of parameter selection mentioned above:

Hardening Soil model with Small-strain Stiffness

For the HS-small model results, Table 4 provides the maximum ground settlements at the 6 monitoring cross sections of DOT tunnel. For comparison, Table 4 also includes the maximum ground settlements from the Mohr-Coulomb model analysis and in-situ monitoring data. With Sec 1-1 as the example, the results of HS-small and Mohr-Coulomb models as well as the in-situ monitoring data are plotted in Fig. 6. The figure shows that the HS-small and Mohr-Coulomb models produced similar trends and points of inflection (the point with the largest slope) for ground settlement troughs. However, the ground settlement trough of the HS-small model was flatter with more distinct convergence. There were no irregular ups and downs observed despite slight bulging of the ground.

Table 4. Max. Ground Settlement by HS-small and MC Model Analysis vs. In-situ Monitoring Data

Monitoring Cross Section	Soil Type	Soil cover depth at center of tunnel (m)	Groundwater level depth (m)	HS-small model (mm)	Mohr-Coulomb model (mm)	In-situ Monitoring (mm)
Sec 1-1	SM,CL	20.60	3.0	22.5	22.5	22.5
Sec 2-2	ML,CL	27.37	2.7	91.6	93.3	91.8
Sec 3-3	SM	27.37	3.0	40.7	41.9	41.3
Sec 4-4	SM	26.77	4.5	27.7	27.3	26.9
Sec 5-5	CL,SM	24.10	3.4	48.7	50.5	50.2
Sec 6-6	CL,SM	19.67	7.2	45.1	43.4	43.0

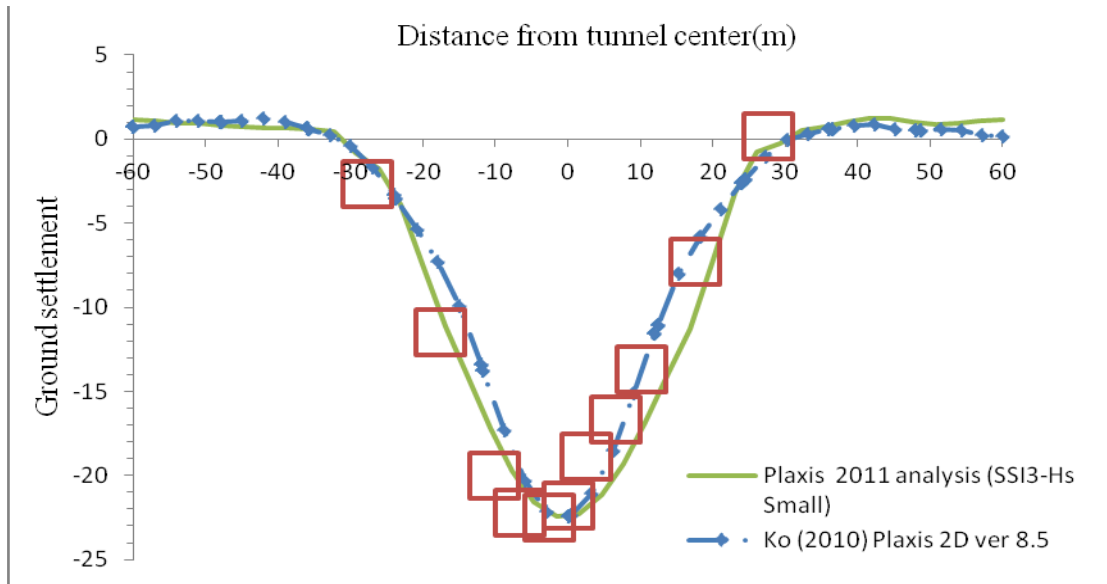


FIG. 6. Ground settlement results at sec 1-1 from HS-small model, MC model and in-situ monitoring

Soft Soil Creep Model Analysis

Soft Soil Creep model features simulation of settlement with time. The ground settlement caused by shield tunneling proposed by Hwang et al. (1997) was introduced. The time history curve of settlement consists of three phases, immediate settlement, consolidation settlement and secondary compression. The analysis was performed for 10 days, 100 days and 365 days, and the maximum ground settlements in each of the time-history phases at the 6 cross sections and the in-situ monitoring data are provided in Table 5 and Fig. 7. With Sec 1-1 as the example, the transverse ground settlements of each of the time-history phases were plotted in Fig. 8. The comparison of analysis result and in-situ monitoring data showed approximate consistency between ground settlement curves. However, apparently large settlement and range of settlement were observed on both side of the center of tunnel in the numeric analysis.

Table 5. Maximum Ground Settlements at Each of the Time-History Phases in the Soft Soil Creep Analysis

Monitoring Cross Section	Soil Type	Soil cover depth at center of tunnel (m)	Groundwater level depth (m)	10~12 days Settlement (mm)	100~104 days Settlement (mm)	175~365 days Settlement (mm)
Sec 1-1	SM,CL	20.60	3.0	22.5	23.9	19.4
Sec 2-2	ML,CL	27.37	2.7	89.9	94.0	95.1
Sec 3-3	SM	27.37	3.0	36.8	39.4	40.1
Sec 4-4	SM	26.77	4.5	26.6	27.5	28.3
Sec 5-5	CL,SM	24.10	3.4	38.0	51.6	52.5
Sec 6-6	CL,SM	19.67	7.2	42.5	45.7	46.3

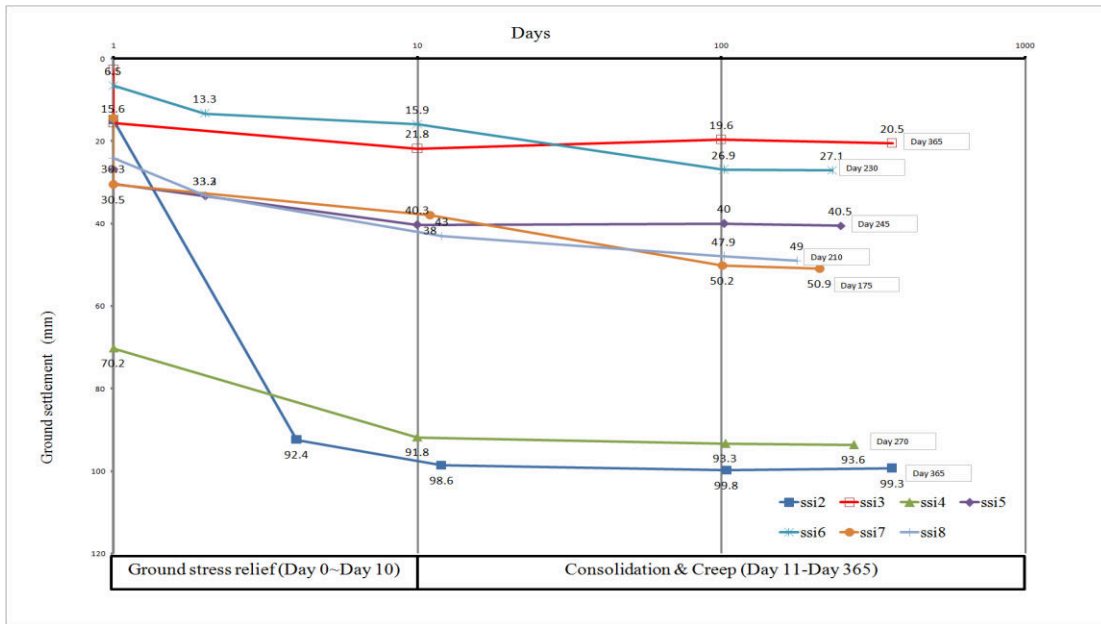


FIG. 7. Time history curves of maximum ground settlement at each of the monitoring cross section

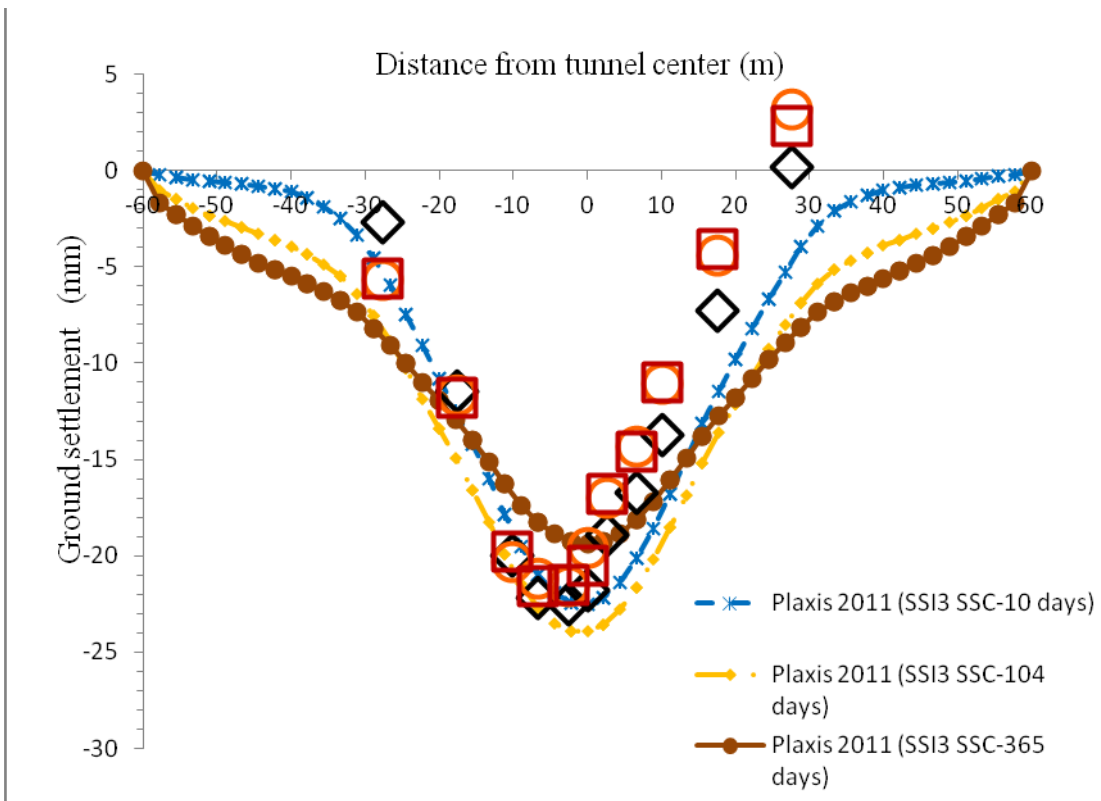


FIG. 8. Transverse ground settlements at sec 1-1 in each of the cross sections vs. in-situ monitoring data

CONCLUSIONS

Hardening Soil model with small-strain stiffness and Soft Soil Creep models were used for numeric analysis and the results were compared with those of Mohr-Coulomb model analysis and in-situ monitoring data to reach the following conclusions:

- (1) The Hs-small, SSC and Mohr-Coulomb models are all applicable for the ground settlement analysis of DOT shield tunnel. The difference between the numeric analysis result and in-situ monitoring data is expected to be insignificant provided that the DOT shield tunneling is going well and the construction site management is appropriate.
- (2) The ground settlement troughs and points of inflection produced from the HS-small model and Mohr-Coulomb model appear to be similar. However, the ground settlement trough of the HS-small model was flatter with more distinct convergence on both sides of the centerline of tunnel. In general, for the shield tunneling in soft soil, the ground settlement is better predicted with the Hs-small model than the Mohr-Coulomb model.
- (3) The ground settlement time-history curve produced from SSC model is largely similar to the in-situ monitoring data. The SSC analysis results and in-situ monitoring data show that a large part of the ground settlement observed in this case is immediate settlement, accounting for 85%, and the other 15% is consolidation and secondary settlement. It is possibly related to the local geology of construction site and the construction works performed.

REFERENCES

- Yu-Syuan Wei (2013), "Simulation Analysis on Ground Settlement and Creep due to Double-O-Tube Shield Tunneling— A Case Study of Airport Access MRT," Master Degree Dissertation, National Taipei University of Technology, Taipei, Taiwan (in Mandarin).
- Brinkgreve, R.B.J. (2011), "Material models manual of Plaxis 2D," *Delft University of Technology & Plaxis bv, the Netherlands*.
- Meen-Wah Gui, Shong-Loong Chen (2013), "Estimation of transverse ground surface settlement induced by DOT shield tunneling," *Tunnelling and Underground Space Technology*, Vol. 33: pp119-130.
- Wan-yi Ke (2011), "Ground surface settlement of Double-O-Tube shield Tunnel for airport access MRT in Taipei basin," Master Degree Dissertation, National Taipei University of Technology, Taipei, Taiwan (in Mandarin).
- Nan-Huei Hwang, Yi-Shiam Hwang (1997), "Ground surface settlement of shield tunneling," *Sino-Geotechnicals*, Vol. 60: pp45-55 (in Mandarin).

Segment Stress Responses of Shield Tunnels caused by Deep Excavations in Improved Soil

ShongLoong Chen¹, Chia-pang Cheng²,

¹ Professor, Graduate Institute of Civil and Disaster Prevention Engineering, National Taipei University of Technology, 1, Sec. 3, Zhongxiao E. Rd., Taipei, 10608, Taiwan. E-mail: fl0391@ntut.edu.tw

² PhD student, Graduate Institute of Civil and Disaster Prevention Engineering, National Taipei University of Technology, 1, Sec. 3, Zhongxiao E. Rd., Taipei, 10608, Taiwan. E-mail: cheng.jiabang@gmail.com

ABSTRACT: A case study on an existing tunnel was investigated in Taipei city. Ground improvement was carried out prior to the excavation of a new underpass crossing over the tunnel. Monitoring systems such as strain gauges and convergent points were set up for the tunnel as excavation for the underpass might cause heaving of the tunnel. The real-time monitoring system has proved to be effective in warning and preventing disaster from happening during the excavation process. Finite difference code FLAC was used to simulate the whole construction sequence and good agreement was obtained between the numerical and field measured results.

INTRODUCTION

A new pedestrian underpass around the new Banqiao main station in New Taipei City, was needed to stride over an existing CP264 MRT tunnel (see Fig.1). In order to install the new underpass and to prevent heaving damages of the MRT tunnel, the ground improvements were carried out before the excavation in progress. The MRT tunnel has an outer diameter of 6 m and a lining thickness of 0.25m. The concrete strength is taken to be 42Mpa. Tunnels were installed approximately 11.3m below the ground surface. The new underpass was a reinforced concrete structure with a rectangular section as shown in Figure 2. It was installed approximately at 9m above the existing tunnels. The excavation section was about 8m deep and 8.6m wide. The support systems were used by the Pack-In-Place-Pile Walls with 16m deep and 60cm in diameter, and two layers of temporary steel props. In order to prevent the heaving of the existing MRT tunnel due to the excavation, the soil improvements, a 4.95m thick of the high pressure jet grouting and a 4.3m thick of low pressure jet grouting, were carried out above the tunnels before the excavation in progress. The design details are shown in Fig.2.

The study simulates excavations for each stage, and analyzes stress variations of segmental tunnel linings with and without ground improvement, through FLAC

software and its inner built Mohr-coulomb stress-strain model, and compare with the recorded data recorded by monitoring system.

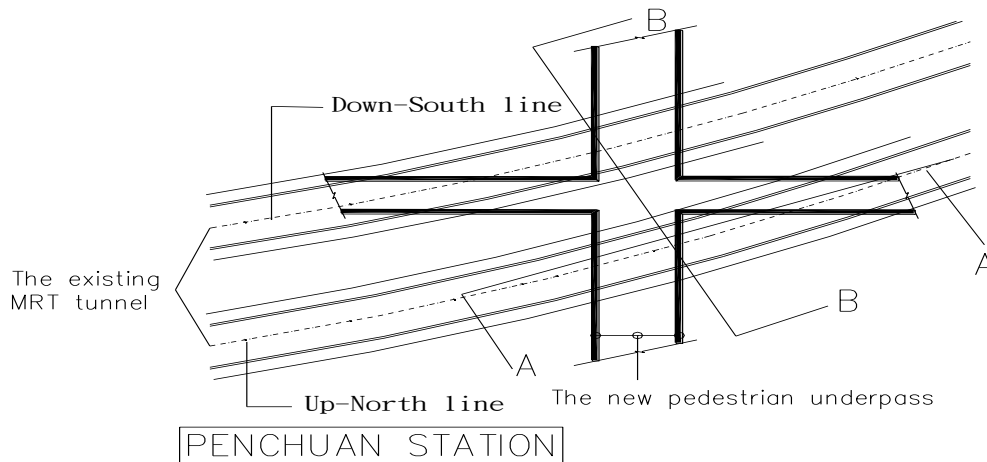


FIG. 1. The plan of pedestrian underpass cross CP264 MRT tunnel.

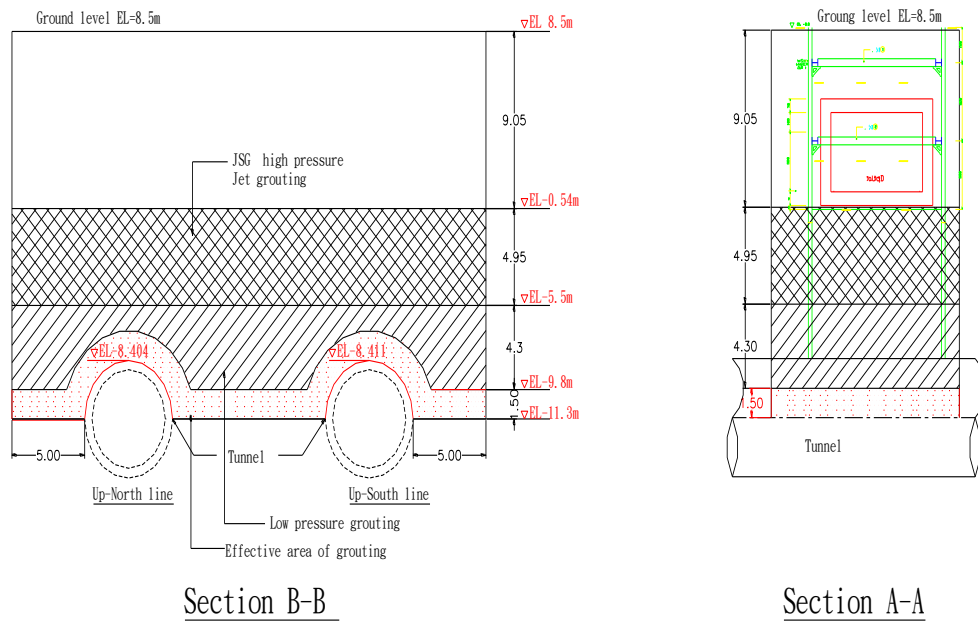


FIG. 2. Profiles of the new underpass and the existing tunnel.

Model Description

The numerical model is based on the two-dimensional explicit finite difference code FLAC (Cundall et al 1993), with the assumption of an ideal elasto-plastic (Mohr-Coulomb) failure criteria. The mesh has a width of 1m and a height of 1m in the central zone and 2m by 1m in both far sides, with 100m by 60m zones in X and Y directions respectively. Fig.3 and 4 show the general arrangement of the analysis cross-section.

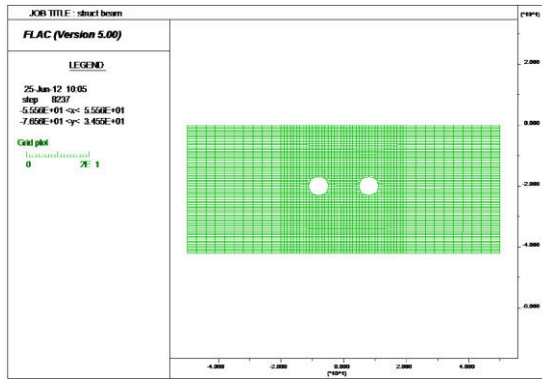


FIG. 3. Grids for initial condition.

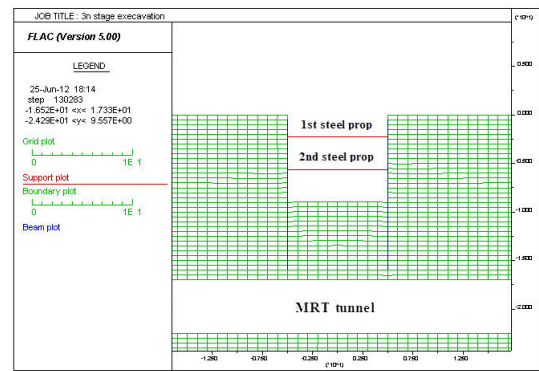


FIG. 4. Prop and excavation – stage 3.

Soil parameters

For this project, the high pressure jet grouting was carried out for 9M~15M below ground surface (3rd layer of CL). The unconfined compression of the improved soil is adopted by 3Mpa. According to Fang’s research, the Poisson’s ratio is between 0.12 and 0.25 in Taipei, Young’s Modulus E50 between 1.11~4.77Gpa. The cohesion C value is considered as $q_u/5$ (JSG 1986). The soil unit weight is increased as 20 percent after improvement (suggested by Jau). For the parameters for the improved soil of this layer, the Poisson’s ratio μ is adopted as 0.2, Young’s Modulus E50 as 3,000,000 kN/m^2 , the cohesion C as 0.6 Mpa. The values of soil unit weight γ_t are obtained by the experimental results. Table 1. shows the values of the soil parameters.

Table 1. Soil parameters

Number of soil	Soil classification	Depth (GL-m)	γ_t (kN/M^3)	C' (kN/M^2)	ϕ	Elastic Modulus E50 (kN/M^2)	Poisson's ratio(μ)	Bulk Modulus B (kN/M^2)	Shear Modulus G (kN/M^2)
1	SF/CL	3.5	18.5	0	32	3500	0.45	11670	1210
2	SM	9	19.1	0	34	12300	0.30	10250	4730
3 (soil unimproved)	CL	15	19.2	2.0	34	15000	0.45	50000	5170
3a (soil improved)	CL	15	23.0	600	34	3000000	0.2	1700000	1250000
4	SM	18	19.1	0	34	16300	0.30	13580	6270
5	CL	21	19.5	6.0	35	22000	0.45	73330	7590
6	SM	28	19.5	0	35	21100	0.3	17580	8120
7	CL	37	19.4	0	34	34000	0.45	113330	11720
8	SM	49	20.0	0	36	34700	0.30	28920	13350
9	GM	60	23.4	0	40	--	--	--	--

Parameters for pack-in-place-pile support walls, segmental tunnel lining and temporary props

Permanent PIP walls and Segmental tunnel lining and temporary steel props are all represented by beam elements. The ring of segmental lining with 0.25m thick was modeled by assuming a continuous lining constituted of beam elements with a slightly reduced flexural stiffness. The reduced stiffness is calculated based on Muir Wood

(1975) and caters for the effect of joints, which reduces the overall lining flexural stiffness. Their flexural stiffness is calculated as $E \times I_e$.

$$E=15000\sqrt{f'c} \tag{1}$$

$$I_e=I_j+\left(\frac{4}{n}\right)^2 I \tag{2}$$

Table 2. Parameters of structural elements

	cross-section (m ² /m)	Elastic Modulus (kN/m ²)	Moment of inertia (m ⁴ /m)	Preload (kN/m)
Tunnel wall	0.205	3.074×10 ⁷	9.53×10 ⁻⁴	--
PIP walls	0.6	1.64×10 ⁷	1.8×10 ⁻³	--
1 st steel prop	2.995×10 ⁻⁵	2.04×10 ⁸	5.1×10 ⁻⁵	66410
2 nd steel prop	4.3475×10 ⁻⁵	2.04×10 ⁸	1.0075×10 ⁻⁴	96401

Analysis steps

For the case study, the following steps were considered with the Finite Difference Method.

1. Initial stress stage before excavation.
2. Pack-In-Place-Pile walls installation and excavation to 3.8m for stage 1 and temporary prop 1.
3. Excavation to 6.8m for stage 2 and temporary prop 2.
4. Excavation to 10.3m for stage 3.
5. Installation of the pedestrian underpass and refill with soil.

Monitoring system

Many monitor systems were set up for the tunnel such as strain gauges, convergent points since the excavation for the underpass installation may cause the heaving of the tunnel. The monitor systems were set up as shown in Fig.5. The locations of installed strain gauges are shows in Fig.6. Compared with experimental results, the numerical analysis has a good prediction. The readings of the strain gauges, which were installed on the segmental tunnel lining, were periodically read and stored in computer automatically. The real-time monitoring system gave very helpful information during the excavation in progress. During the construction stages, the stress variations of segmental lining showed the critical values for several times as the high pressure jet grouting proceeds prior to excavation. As soon as the warning situations happen, the constructor stops and decreases the pressure for the jet grouting immediately. Actions should be taken as the warning values are shown on the real-time monitor. Fortunately, there were no any damages for the tunnel during the excavation in progress for the new underpass installation. The warning system provides a successful tool, not only during the high pressure jet grouting in progress but also the excavation process.